Electrophoresis of composite soft particles with differentiated core and shell permeabilities to ions and fluid flow

Saurabh Maurya, Partha Gopmandal, Hiroyuki Ohshima, Jérôme F.L. Duval

▶ **To cite this version:**

Saurabh Maurya, Partha Gopmandal, Hiroyuki Ohshima, Jérôme F.L. Duval. Electrophoresis of composite soft particles with differentiated core and shell permeabilities to ions and fluid flow. Journal of Colloid and Interface Science, 2020, 558, pp.280-290. 10.1016/j.jcis.2019.09.118 . hal-02351029

HAL Id: hal-02351029

https://hal.univ-lorraine.fr/hal-02351029

Submitted on 6 May 2020

HAL is a multi-disciplinary open access archive for the deposit and dissemination of scientific research documents, whether they are published or not. The documents may come from teaching and research institutions in France or abroad, or from public or private research centers.

L'archive ouverte pluridisciplinaire **HAL**, est destinée au dépôt et à la diffusion de documents scientifiques de niveau recherche, publiés ou non, émanant des établissements d'enseignement et de recherche français ou étrangers, des laboratoires publics ou privés.

Graphical Abstract

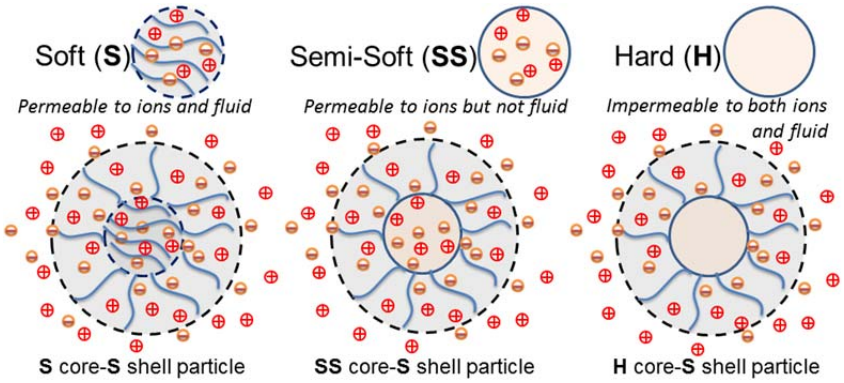

Electrophoresis of Composite Soft Particles with Differentiated Core and Shell Permeabilities to Ions and Fluid Flow

Saurabh K. Maurya[a], Partha P. Gopmandal[b*], Hiroyuki Ohshima[c], Jérôme F.L. Duval[d]

[a] Department of Mathematics, National Institute of Technology Patna, Patna-800005, India.
[b] Department of Mathematics, National Institute of Technology Durgapur, Durgapur-713209, India.
[c] Faculty of Pharmaceutical Sciences, Tokyo University of Science Noda, Chiba, Japan.
[d] CNRS, Université de Lorraine, Laboratoire Interdisciplinaire des Environnements Continentaux (LIEC), UMR 7360 CNRS-Université de Lorraine, F-54500 Vandoeuvre-lès-Nancy, France.

[*]**Corresponding Author.** Email: partha.gopmandal@maths.nitdgp.ac.in. Phone:+91-7250276690.

Abstract

Within the framework of analytical theories for soft surface electrophoresis, soft particles are classically defined by a hard impermeable core of given surface charge density surrounded by a polyelectrolyte shell layer permeable to both electroosmotic flow and ions from background electrolyte. This definition excludes practical core-shell particles, *e.g.* dendrimers, viruses or multi-layered polymeric particles, defined by a polyelectrolytic core where structural charges are distributed and where counter-ions concentration and electroosmotic flow velocity can be significant. Whereas a number of important approximate expressions has been derived for the electrophoretic mobility of hard and soft particles, none of them is applicable to such generic composite core-shell particles with differentiated ions- and fluid flow-permeabilities of their core and shell components. In this work, we elaborate an original closed-form electrophoretic mobility expression for this generic composite particle type within the Debye-Hückel electrostatic framework and thin double layer approximation. The expression explicitly involves the screening Debye layer thickness and the Brinkman core and shell hydrodynamic length scales, which favors so-far missing analysis of the respective core and shell contributions to overall particle mobility. Limits of this expression successfully reproduce results from Ohshima's electrophoresis theory solely applicable to soft particles with or without hard core.

Keywords: Electrophoretic mobility, Electrophoresis, Soft particles, Core-shell particles, Polyelectrolyte layers, Permeabilities to ions and fluid flow, Thin double layer theory, Poisson-Boltzmann equation.

1. Introduction

Electrophoresis is a well-established technique for addressing the electrostatic properties of abiotic and biotic colloidal particles in aqueous solution [1-2]. Pending proper conversion of the measured electrophoretic mobility into relevant particle electrostatic descriptors, electrophoresis provides a way to capture how electrostatics contributes to (bio)particles stability against aggregation [2-3], how it impacts (or not) nanoparticle-cell, cell-cell or nanoparticle-functionalized surface interactions [4-6], the attachment of bacteria to surfaces [7-9], the binding of metal ions to (nano)particles [10-12], the transport of particles in porous media [13-15], the accumulation of metal ions in microorganisms [16] or even the response of bioluminescent metal-sensing bacterial reporters [17-18]. Quantitative interpretation of electrophoretic mobility data and subsequent evaluation of the defining particle electrostatic features differ according to the type of particles examined, in particular the magnitude of their permeability to electrolyte ions and to the (electroosmotic) flow developed under electrokinetic conditions. For impermeable **hard** particles, a slip plane can be properly identified and the electrophoretic mobility converted into zeta-potential value [2, 19-20] by means of theoretical expressions that integrate hydrodynamic retardation effects, surface conduction, and/or electric double layer polarization depending on magnitude of particle surface charge, on particle size and on electrolyte concentration in solution [2, 19-24]. Unlike hard particles, **soft** colloids harbor an ion- and flow-penetrable charged polymer surface layer that decorates an impermeable core (so-called core-shell particles) [1, 25]. Soft particles also include colloids consisting of a permeable polymeric material in the absence of intraparticulate core component (so-called porous particles) [25]. Paradigms of systems whose electrophoresis behavior relates to that of soft particles include polyelectrolyte particles [26-28], bacteria [1, 17-18, 29-31], viruses [32-33], (bio)functionalized, thermo- and/or iono-responsive (nano)particles [34-36], recombinant protein particles [37], environmental particles like humic substances [38], and polyelectrolyte multi-layered particles [39-40], to quote only a few. It has long been recognized that the electrophoretic properties of soft particles deviate substantially from that of hard particles and that the concept of zeta-potential is inapplicable to soft particles for which the gradual suppression of the electroosmotic flow profile within the permeable component renders impossible any *a priori* definition of a slip plane [1, 25, 41-42]. A variety of soft surface electrokinetic models have therefore been reported to provide a quantitative connection between electrophoretic mobility and electrostatic features of soft particles (see [1, 25, 41-42] and references therein). The models differ according to their treatment of particle electrostatics based on linear or non-linear Poisson-Boltzmann theory, to their account or not of double layer polarization, to their integration or not of inhomogeneous distribution of structural charges within the soft particle body and to the boundary conditions adopted at the very core/surface layer interface [41-58]. Various approximate analytical expressions have been derived for the electrophoretic mobility of soft particles, in particular by

Ohshima and colleagues [25, 43-47, 51-55], essentially under conditions where electric double layer polarization by the applied electric field is insignificant. Despite their inherent limitations connected to the approximations adopted, these expressions have the merit to be tractable analytically and to make explicit how particle electrophoretic mobility is impacted by solution salinity and by the key electro-hydrodynamic determinants of the soft particles, which includes the density of charges they carry and their so-called hydrodynamic softness identified with the reciprocal of the hydrodynamic penetration (Brinkman) length scale [59]. Numerous examples reported in literature illustrate the successful applications of such equations to interpret electrophoresis data measured *e.g.* on biological cells or engineered nanoparticles at sufficiently large electrolyte concentrations [29, 30, 60-65].

The term 'permeability' adopted within soft surface electrokinetic literature generally applies to particulate systems penetrable to both ions and liquid flow [25]. Other colloids, termed as **semi-soft** particles by Ohshima [54], may be permeable to electrolyte ions but not to flow. Such a disparity between macroscopic flow and ion transport is not rare and has been commented by Lyklema in his seminal discussion of the structure of 'stagnant layers' and of surface conduction occurrence behind the shear plane in the context of hard particles electrokinetics [22, 66-67]. In particular, Lyklema argued that 'a few percent of a gelling agent may fully immobilize liquid [in gels] (on a macroscopic scale) without materially suppressing self-ion diffusion (a molecular process)' [67]. Electrokinetics of semi-soft particles still deviate from that of hard particles as their outer surface potential remains inherently determined by structural charges distributed over the particle body volume [39, 54]. Examples of semi-soft particles are hyper-branched nano-dendrimers with zwitterionic functionality [39], whose electrophoretic features were recently shown to comply with numerical theory for diffuse soft particles in the limit of infinite hydrodynamic softness [39, 58], and various bacterial strains displaying sub-nanometric hydrodynamic flow penetration in their surface structures that may significantly protrude towards the outer aqueous medium [1]. In turn, the above differentiation between soft (**S**) and semi-soft (**SS**) particles -*i.e.* that between particles permeable to ions **and** to fluid flow, and particles permeable to ions **but not** to fluid flow, respectively- asks for the so-far missing derivation of tractable analytical expressions relevant for the electrophoretic mobility of practical core-shell particles where polyelectrolytic core (**c**, in short) and shell layer (**sl**, in short), made of distinct materials, differ according to their respective propensity to host electrolyte ions and/or fluid flow. This is the purpose of this work where we tackle the situations of dilute dispersions of particles defined by (i) soft core and soft shell, (ii) semi-soft core and soft shell, and (iii) semi-soft core and semi-soft shell components. To lighten notations, particles of type (i), (ii) and (iii) above are termed hereafter **Sc-Ssl**, **SSc-Ssl** and **SSc-SSsl** particles. The work extends previous analytical theory by Ohshima solely applicable to particles where soft [25, 51-54] or semi-soft [54] shell decorates a strictly hard core, impermeable to both ions and fluid flow. The various types of particles considered in

this work are further defined in **Table 1**. Mobility expressions of Sc-Ssl, SSc-Ssl and SSc-SSsl particles are elaborated here within the framework of the Debye-Hückel and thin double layer approximations valid for poorly to moderately charged particles whose radius well exceeds Debye layer thickness. As a result, the here-derived particle mobility expressions are applicable at sufficiently large electrolyte concentrations. It is shown that appropriate limits of the obtained expressions correctly reduce to previous results obtained by Ohshima [25, 51-54] valid for colloids comprised of a hard core surrounded by a soft or semi-soft shell layer (**Table 1**).

The merit of this work is therefore the elaboration of an original analytical expression for the electrophoretic mobility of **the very generic type** of core-shell particles where both core and shell components are defined by distinct permeabilities to ions from background electrolyte *and* to electroosmotic flow. Paradigms of such particles include dendrimers [39], viruses [32], multilayered particles [40] or bacteria decorated by protruding soft surface appendages [1]. There is a large amount of expressions derived in literature [25, 51-54] (mostly by Ohshima), but none of them is applicable to this generic type of composite soft particles with differentiated ions and fluid flow permeabilities, as considered in our analysis. The analytical expressions so far available in literature solely involve the electrohydrodynamic properties of the only particle shell component but discard systematically the defining electrostatic *and* hydrodynamic properties of the particle core region. The elaboration of an explicit analytical expression that correctly integrates the defining electro-hydrodynamic features **of both** core and particle shell compartments is most timely as it should help experimentalists analyze electrokinetic results (collected at sufficiently large electrolyte concentrations where linearization of Poisson-Boltzmann equation is legitimate) with a proper account of the complex core-shell structure of the investigated particulate systems. Such analyses are relevant for deriving electrostatic and structural descriptors of particles and to interpret *e.g.* particle/surface electrostatic interactions [6], particle swelling/shrinking processes [34], or binding of nanoparticles to biological cells [4]. Various limits of our mobility expression derived for **specific** ranges of core diameter, shell dimension, electrolyte concentration and magnitude of flow permeabilities, are shown to recover previous approximate results from literature [25, 51-54].

CORE-SHELL PARTICLE type	CORE		SHELL	
	Permeability to ions	Permability to fluid flow	Permeability to ions	Permability to fluid flow
Sc-Ssl (any ρ_{core} , $1/\lambda_c \neq 0$; any ρ_{shell} , $1/\lambda_{sl} \neq 0$)	YES	YES	YES	YES
SSc-Ssl (any ρ_{core} , $\lambda_c \to \infty$; any ρ_{shell} , $1/\lambda_{sl} \neq 0$)	YES	NO	YES	YES
Hard core-Ssl [25, 51-54] (any ρ_{core} , $\lambda_c \to \infty$; any ρ_{shell} , $1/\lambda_{sl} \neq 0$)	NO	NO	YES	YES
Hard core-SSsl [54] (any ρ_{core} , $\lambda_c \to \infty$; any ρ_{shell} , $\lambda_{sl} \to \infty$)	NO	NO	YES	NO
SSc-SSsl (any ρ_{core} , $\lambda_c \to \infty$; any ρ_{shell} , $\lambda_{sl} \to \infty$)	YES	NO	YES	NO

Table 1: Differentiated types of composite semi soft (SS)-soft (S) particles consisting of a polyelectrolyte core (c) decorated by a polyelectrolyte shell layer (sl). Electrophoretic mobility expressions of hard core-soft shell and hard core-semi soft shell particles are provided by Ohshima in [25, 51-54] and [54], respectively, with a particle core component that carries surface charges (*i.e.* charges that are not distributed all over the core volume, a situation that is specifically tackled in this work). Hard particles are defined by particle core and shell components that are both impermeable to ions and fluids flow (not mentioned in this table). The expressions elaborated in this work for the electrophoretic mobility of **Sc-Ssl**, **SSc-Ssl**, **hard core-Ssl**, **hard core-SSsl** and **SSc-SSsl** composite particles are defined by Eqs. (28),

(36), (37), (39) and (40), respectively. The operative conditions in terms of charge densities in the particle core and shell layer (ρ_{core} and ρ_{shell} , respectively) and of fluid flow permeabilities in these particle compartments (λ_c and λ_{sl} , respectively) are further specified in Table 1.

2. Results and discussion.

2.1. Setting the stage.

In the developments that follow, we consider Sc-Ssl, SSc-Ssl and SSc-SSsl particle types (see **Table 1**) in the limit where particles curvature is immaterial in defining the electric double layer (EDL) field at the particle/solution interface. This situation is met in the thin EDL limit where particle radius is much larger than the Debye layer thickness, denoted as $1/\kappa$. A scheme of the core-shell particles viewed in this flat-plate representation is given in **Figure 1**, which further specifies the nomenclature adopted. The particle core then assimilates with a polyelectrolyte layer (PEL in short) of thickness L and the peripheral particle shell with a PEL of thickness d (**Figure 1**). The core and shell PELs both carry structural charges with densities denoted as ρ_{core} and ρ_{shell} defined by $\rho_{core} = z_c F N_c$ and $\rho_{shell} = z_{shell} F N_{shell}$, where

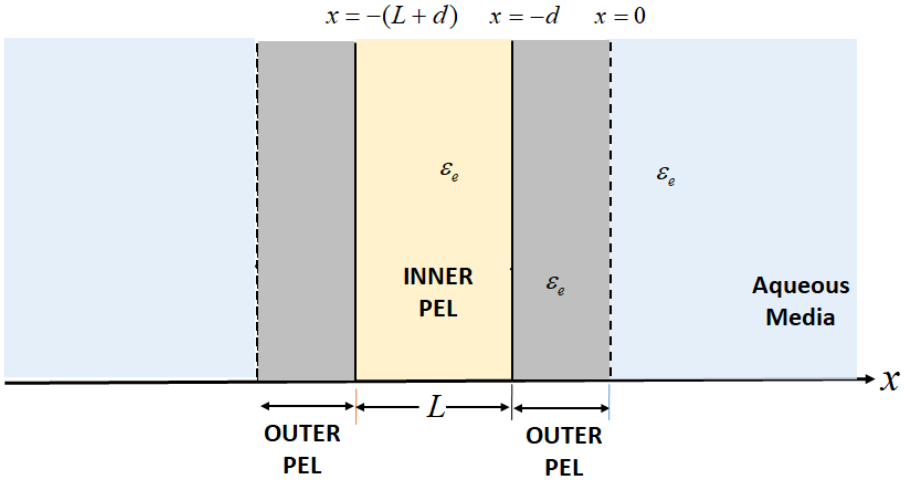

Fig. 1. Schematic illustration of a core-shell particle consisting of an inner polyelectrolyte layer (PEL in short) of thickness L (core component) covered by a peripheral PEL (shell component) of thickness d. Details on the adopted nomenclature are provided.

F is the Faraday constant, z_c, N_c and z_{shell}, N_{shell} are the valence and molar concentration of the ionogenic functional groups distributed within the inner core and outer shell PELs, respectively. Depending on the chemistry of the particulate system considered, the densities of charges ρ_{core} and ρ_{shell} may be formulated as a function of solution pH pending proper account of the dissociation of the functional groups on salt concentration (or, equivalently, on particle electrostatics), as detailed along the

lines given elsewhere [12, 34, 39]. The water contents in the core and shell PELs are here sufficiently large for the dielectric permittivity ε_e therein to identify with that in the outer aqueous solution [58, 68]. In the next section, the governing equations for the electrophoresis of the various types of core-shell particles of interest are elaborated under dilute dispersion conditions (*i.e.* at sufficiently low particle volume fractions in line with the absence of particle-particle electro-hydrodynamic interactions) in a background electrolyte containing cations of valence z_+ and bulk number concentration n_+^∞ (in m^{-3}) and anions with valence z_- and bulk number concentration n_-^∞ (in m^{-3}). Realizing that the case of semi-soft core-soft shell (SSc-Ssl) and semi-soft core-semi-soft shell (SSc-SSsl) particles (**Table 1**) are limits of the more general situation where both particle core and shell components are permeable to ions **and** fluid flow (Sc-Ssl particles, **Table 1**), flow field and electrostatic potential distributions are first determined for this latter generic particle type.

2.2. Theory for evaluation of electroosmotic flow field and electrostatic potential distributions in soft core-soft shell (Sc-Ssl) particles

2.2.1. Electroosmotic flow field distribution inside- and in the vicinity of a Sc-Ssl particle.

Considering the case of Sc-Ssl particles (**Table 1**), the distribution of the electroosmotic flow (EOF in short) field u in the direction x perpendicular to the particle/solution interface (**Figure 1**) subjected to an applied electric field of magnitude E is determined by the Darcy-Brinkman and Stokes equations according to

$$\eta\frac{\mathrm{d}^2u}{\mathrm{d}x^2}-\gamma_c u(x)+\rho_e E=0 \qquad :-\left(\frac{L}{2}+d\right)\le x<-d \tag{1}$$

$$\eta\frac{\mathrm{d}^2u}{\mathrm{d}x^2}-\gamma_{sl} u(x)+\rho_e E=0 \qquad :-d\le x<0 \tag{2}$$

$$\eta\frac{\mathrm{d}^2u}{\mathrm{d}x^2}+\rho_e E=0 \qquad :x\ge 0 \tag{3}$$

, where η is the dynamic fluid viscosity, γ_c and γ_{sl} are the coefficients of friction exerted by the inner core and outer shell on the flow, respectively, and $-\gamma_{c,sl}u(x)$ are the corresponding frictional forces. The friction coefficients γ_c and γ_{sl} are related to the hydrodynamic softnesses λ_c and λ_{sl} (in m^{-1}) of the core and shell particle components, respectively, *via* the relationships $\lambda_{c,sl}=\sqrt{\gamma_{c,sl}/\eta}$ [25]. The term $\rho_e E$ in Eqs. (1-3) represents the electromotive force due to the electric field applied in the x-direction

and which causes electrophoretic particle motion. The net charge density ρ_e of mobile ions at position x across the particle/solution interface is defined by $\rho_e(x) = z_+ e n_+(x) + z_- e n_-(x)$, where e is the elementary charge, and $n_{+,-}(x)$ are the local concentration of cations (+) and anions (-) that obey Boltzmann statistics

$$n_{+,-}(x) = n_{+,-}^{\infty} \exp\left[-\frac{z_{+,-} e\psi(x)}{k_B T}\right] \tag{4}$$

, where $\psi(x)$ is the electric potential at position x, $k_B T$ is the thermal energy and $n_{+,-}^{\infty}$ represent the bulk number concentrations of cations and anions (in m^{-3}). The boundary conditions verified by u are given by

$$\left.\frac{du}{dx}\right|_{x=-(L/2+d)} = 0 \tag{5}$$

$$u(-d^-) = u(-d^+) \tag{6}$$

$$\left.\frac{du}{dx}\right|_{x=-d^-} = \left.\frac{du}{dx}\right|_{x=-d^+} \tag{7}$$

$$u(0^-) = u(0^+) \tag{8}$$

$$\left.\frac{du}{dx}\right|_{x=0^-} = \left.\frac{du}{dx}\right|_{x=0^+} \tag{9}$$

$$u \to -U_E \quad \text{as} \quad x \to \infty \tag{10}$$

, where Eq. (5) reflects flow symmetry at $x = -(L/2 + d)$ and Eqs. (6)-(9) translate the required continuity of the field and its derivative at the core/shell and shell/solution interfaces (**Figure 1**). Eq. (10) indicates that under steady-state conditions the electroosmotic flow velocity (in magnitude) far from the particle necessarily identifies with particle electrophoretic velocity whose magnitude is denoted as U_E. Explicit evaluation of the electroosmotic flow profile defined by Eq. (1-3) and by the boundaries (5)-(10) requires knowledge of the potential distribution $\psi(x)$. This is done below for situations where both particle core and particle shells are permeable to ions (relevant for Sc-Ssl, SSc-Ssl, SSc-SSsl particle types, **Table 1**) and for cases where the particle inner core, defined by a density of charges distributed all over its volume, is not penetrable by ions (as applicable for hard core-Ssl, hard core-SSsl particles, **Table 1**).

2.2.2. Electrostatic potential distribution within and outside particles with ion-penetrable core and shell components.

Under the examined conditions where core and shell particle regions are both penetrable by ions from the background electrolyte, the position-dependence of the potential $\psi(x)$ is governed by the Poisson-Boltzmann equation written within the Debye-Hückel approximation in the core and shell particle domains according to

$$\frac{\mathrm{d}^2\psi}{dx^2} = \kappa^2\psi - \frac{\rho_{core}}{\varepsilon_e} \qquad : -\left(\frac{L}{2}+d\right) \le x < -d \tag{11}$$

$$\frac{\mathrm{d}^2\psi}{dx^2} = \kappa^2\psi - \frac{\rho_{shell}}{\varepsilon_e} \qquad : -d \le x < 0 \tag{12}$$

$$\frac{\mathrm{d}^2\psi}{dx^2} = \kappa^2\psi \qquad : x \ge 0 \tag{13}$$

, which applies to a symmetrical $z:z$ background electrolyte with $z_+ = -z_- = z$, $n_+^\infty = n_-^\infty = n_\mathrm{o}^\infty$ and the reciprocal of the Debye layer thickness is defined by $\kappa = \sqrt{2z^2e^2n_\mathrm{o}^\infty / \varepsilon_e k_B T}$. The required boundary conditions associated to Eqs. (11)-(13) are derived from symmetry of the potential profile at the position $x = -(L/2+d)$ (Eq. (14)), by the potential and field continuity conditions at $x = 0$ and $x = -d$ (Eqs. (15)-(18)), and finally by the vanishing of the potential and electric field far from the particle at $x \to \infty$ (Eq. (19)) (**Figure 1**), *i.e*.

$$\left.\frac{\mathrm{d}\psi}{\mathrm{d}x}\right|_{x=-(L/2+d)} = 0 \tag{14}$$

$$\psi(-d^-) = \psi(-d^+) \tag{15}$$

$$\left.\frac{\mathrm{d}\psi}{\mathrm{d}x}\right|_{x=-d^-} = \left.\frac{\mathrm{d}\psi}{\mathrm{d}x}\right|_{x=-d^+} \tag{16}$$

$$\psi(0^-) = \psi(0^+) \tag{17}$$

$$\left.\frac{\mathrm{d}\psi}{\mathrm{d}x}\right|_{x=0^-} = \left.\frac{\mathrm{d}\psi}{\mathrm{d}x}\right|_{x=0^+} \tag{18}$$

$$\psi(x) \to 0 \ \text{ and } \ \frac{\mathrm{d}\psi}{\mathrm{d}x} \to 0 \ \text{ as } \ x \to \infty \tag{19}$$

At this stage, it is emphasized that the boundaries formulated by Eqs. (14)-(19) are applicable to all types of particles whether their core and shell are permeable or not to electrolyte ions. Eq. (12) may be rewritten in the concise form

$$\frac{\mathrm{d}^2\psi}{dx^2} = \kappa^2(\psi - \psi_{DON}) \qquad : -d \le x < 0 \tag{20}$$

, where we introduced the Donnan potential ψ_{DON} reached in the bulk shell layer at $d >> 1/\kappa$ [69,70], and defined by

$$\psi_{DON} = \frac{\rho_{shell}}{\varepsilon_e \kappa^2} \tag{21}$$

After solving Eqs. (11)-(13) with boundaries defined by Eqs. (14)-(19), the potential distribution operational in the particle core and shell compartments both permeable to ions from background electrolyte, may be recast in the generic final form (**Supplementary Material**)

$$\psi(x) = \begin{cases} \left[\psi(-d) - \dfrac{\rho_{core}}{\varepsilon_e \kappa^2}\right]\mathrm{sech}\left(\dfrac{\kappa L}{2}\right)\cosh\left[\kappa\left(x + \dfrac{L}{2} + d\right)\right] + \dfrac{\rho_{core}}{\varepsilon_e \kappa^2} & : \quad -\left(\dfrac{L}{2} + d\right) \le x < -d \\ \psi_{DON}[1 - \cosh(\kappa x) + P\mathrm{e}^{-\kappa(x+d)}] + Q\dfrac{\rho_{core}}{\varepsilon_e \kappa^2}\mathrm{e}^{-\kappa(x+d)} & : \quad -d \le x < 0 \\ \psi_{DON} P\mathrm{e}^{-\kappa(x+d)} + Q\dfrac{\rho_{core}}{\varepsilon_e \kappa^2}\mathrm{e}^{-\kappa(x+d)} & : \quad x \ge 0 \end{cases} \tag{22}$$

, where P and Q are defined by

$$\begin{cases} P = \left[\dfrac{[\sinh(\kappa d) - \tanh\left(\dfrac{\kappa L}{2}\right)(1 - \cosh(\kappa d))]}{1 + \tanh\left(\dfrac{\kappa L}{2}\right)}\right] \\ Q = \dfrac{\tanh\left(\dfrac{\kappa L}{2}\right)}{1 + \tanh\left(\dfrac{\kappa L}{2}\right)} \end{cases} \tag{23}$$

The expressions of the potentials at the core/shell solution interface $\psi(-d)$ involved in Eq. (22) and at the shell/solution interface, $\psi(0)$, are further defined by

$$\begin{cases} \psi(0) = \left(\psi_{DON} P + Q\dfrac{\rho_{core}}{\varepsilon_e \kappa^2}\right)\mathrm{e}^{-\kappa d} \\ \psi(-d) = \psi_{DON}[1 - \cosh(\kappa d) + P] + Q\dfrac{\rho_{core}}{\varepsilon_e \kappa^2} \end{cases} \tag{24}$$

2.2.3. Electrostatic potential distribution within and outside core-shell particles with ion-impenetrable inner core.

For the classical case of particles with hard core and soft or semi-soft shell component, as introduced by Ohshima [25, 51-54], the inner core compartment is considered to carry surface charges. Corresponding electrostatic descriptor may then be defined in terms of a uniform surface potential or surface charge density while the outer PEL shell carries structural (immobile) charges all over its volume. In the developments below, we derive the electrostatic potential distribution with relaxing the standard condition of charges distribution at the only hard core surface and explore the scenario where such charges are distributed all over the core volume, in addition to shell charges located within the particle surface layer. For such a core-shell particle with ion-impenetrable inner core and ion-penetrable outer PEL (*i.e*. relevant for hard core-Ssl, hard core-SSsl particles, **Table 1**), the counterparts of Eqs. (11)-(13) for the potential distribution are given by Eqs (S6)-(S8) in **Supplementary Material**. Following a strategy similar to that invoked in the previous section (see **Supplementary Material**), after algebraic developments it is shown that the potential distribution within and outside hard core-Ssl and hard core-SSsl particles with volumic core charge density is defined by

$$\psi(x)=\begin{cases} -\dfrac{\rho_{core}}{2\varepsilon_e}\left\{\left(x+\dfrac{L}{2}+d\right)^2-\left(\dfrac{L}{2}\right)^2\right\}+\psi_{DON}(1-\mathrm{e}^{-\kappa d})+\dfrac{\rho_{core}}{2\varepsilon_e\kappa}L & : \quad -\left(\dfrac{L}{2}+d\right)\le x<-d \\ \psi_{DON}[1-\mathrm{e}^{-\kappa d}\cosh\kappa(x+d)]+\dfrac{\rho_{core}}{2\varepsilon_e\kappa}L\mathrm{e}^{-\kappa(x+d)} & : \quad -d\le x<0 \\ \psi_{DON}\mathrm{e}^{-\kappa(x+d)}\sinh(\kappa d)+\dfrac{\rho_{core}}{2\varepsilon_e\kappa}L\mathrm{e}^{-\kappa(x+d)} & : \quad x\ge 0 \end{cases} \tag{25}$$

It is stressed that the Poisson-Boltzmann equation is here explicitly solved in the core particle volume with account of the defining charge density therein whereas a simple boundary condition is commonly considered at the core/shell interface for solving electrostatics. This boundary relates either to the particle core surface potential or to the particle core surface charge density. In the limit $L\to 0$ and $\rho_{core}\to\infty$ with the term $L\rho_{core}/2$ kept constant, $L\rho_{core}/2$ reduces to the core surface charge density $\sigma=\lim_{L\to 0,\rho_{core}\to\infty} L\rho_{core}/2$. In such a situation, the expression of the EDL potential distribution defined by Eq. (25) reduces to the result formulated by Maurya et al. in the Debye-Hückel limit [71] (Eq. (S10) in **Supplementary Material**).

2.2.4. Generic analytical expression for the electroosmotic flow field distribution inside- and in the vicinity of Sc-Ssl particles.

The electroosmotic flow profiles within and outside core-shell particles harboring a soft outer PEL supported by a soft inner PEL (**Table 1**) is provided by Eqs. (1-3) pending replacement therein of $\psi(x)$ by its appropriate defining expression (*i.e.* Eq. (22)). For the case of hard (ions-impermeable) core surrounded by a soft or semi-soft shell component, Eqs. (1-3) remain applicable provided that the potential distribution therein is defined by Eq. (25). It is recalled that the particle electrophoretic velocity is hereafter denoted as U_E (Eq. (10)). Using Eq. (S11) (**Supplementary Material**) that defines the charges density ρ_e involved in Eqs. (1)-(3), and subsequent solving of the flow profile (Eqs. (1)-(3)) subject to the boundaries specified by Eqs. (5)-(10), we obtain after lengthy developments the following expression for $u(x)$ relevant to the case of Sc-Ssl particles

$$u(x)=\begin{cases} C_1\cosh\left[\lambda_c\left(x+\frac{L}{2}+d\right)\right]+\dfrac{\varepsilon_e E}{\eta}\left[\psi(x)+\lambda_c\int_{-\left(\frac{L}{2}+d\right)}^{x}\sinh\left[\lambda_c(x-t)\right]\psi(t)\mathrm{d}t\right]-\dfrac{\rho_{core}E}{\lambda_c^2\eta} & \\ \qquad\qquad : -\left(\dfrac{L}{2}+d\right)\le x<-d & \\ C_2\cosh(\lambda_{sl}x)-\dfrac{\varepsilon_e E}{\eta}\lambda_{sl}\int_{-d}^{0}\sinh(\lambda_{sl}x)\cosh(\lambda_{sl}t)\psi(t)\mathrm{d}t & \\ +\dfrac{\varepsilon_e E}{\eta}\left[\psi(x)+\lambda_{sl}\int_{-d}^{x}\sinh\left[\lambda_{sl}(x-t)\right]\psi(t)\mathrm{d}t\right]-\dfrac{\rho_{shell}E}{\lambda_{sl}^2\eta} & : -d\le x<0 \\ u(0)-\dfrac{\varepsilon_e E}{\eta}\left[\psi(0)-\psi(x)\right] & : x\ge 0 \end{cases} \tag{26}$$

, where the scalar C_1 and C_2 are defined by Eqs. (S13) and (S14) in **Supplementary Material**, respectively. C_1 and C_2 both involve intricate integral expressions of the potential distribution given by Eq. (22). The expression (26) is further used in the sections below to find the searched analytical expressions for the electrophoretic mobility of Sc-Ssl, SSc-Ssl and SSc-SSsl composite particle types (**Table 1**). On the other hand, for core-shell particles with hard inner core, the velocity field may simply be obtained from Eq. (26) taken in the limit $\lambda_c\to\infty$, which provides

$$u(x)=\begin{cases}\dfrac{\varepsilon_e E}{\eta}\left[\psi(x)-\psi(-d)\dfrac{\cosh(\lambda_{sl}x)}{\cosh(\lambda_{sl}d)}+\lambda_{sl}\int_{-d}^{x}\sinh\left[\lambda_{sl}(x-t)\right]\psi(t)\mathrm{d}t\right. \\ \left.-\left\{\dfrac{\lambda_{sl}}{\cosh(\lambda_{sl}d)}\int_{-d}^{0}\cosh(\lambda_{sl}t)\psi(t)\mathrm{d}t\right)\right\}\sinh\left[\lambda_{sl}(x+d)\right]\Bigg] \\ -\dfrac{\rho_{fix}E}{\lambda_{sl}^2\eta}\left(1-\dfrac{\cosh(\lambda_{sl}x)}{\cosh(\lambda_{sl}d)}\right) \qquad : -d\le x<0 \\ u(0)-\dfrac{\varepsilon_e E}{\eta}\left[\psi(0)-\psi(x)\right] \qquad : x\ge 0\end{cases} \tag{27}$$

, where $\psi(t)$ is here defined by Eq. (25). A similar expression of the electroosmotic flow profile is provided by Ohshima [45-46] for the classical (hard) core-(soft) shell particle type. However, the here-reported expression has the merit to involve the appropriate electric double layer potential distribution given by Eq. (25) applicable to the most general scenario where the inner core is defined by a density of charges distributed all over its physical volume.

2.3. Analytical expressions for the electrophoretic mobility of composite semi-soft and soft core-shell particles (see **Table 1**).

The general expression for the electrophoretic mobility of a core-shell particle is defined by $\mu_E=-U_E/E=-u(x\to\infty)/E$ **.** Substituting the potential distribution defined by Eq. (22) into the integral mobility expression derived for **Sc-Ssl** particles in **Supplementary Material** (Eq. (S15)), we find that the electrophoretic mobility of **Sc-Ssl** particles is given by the fully developed expression

$$\mu_E = \frac{\varepsilon_e \psi_{DON}}{\eta}\left[\frac{1}{F_1}\left([1-\cosh(\kappa d)+P]F_2+(\cosh(\lambda_{sl}d)-1)+\frac{\lambda_{sl}^2}{\kappa^2-\lambda_{sl}^2}(\cosh(\lambda_{sl}d)-\cosh(\kappa d))\right)+\right.$$
$$\frac{P\lambda_{sl}^2}{\kappa^2-\lambda_{sl}^2}\frac{1}{F_1}\left\{1-\mathrm{e}^{-\kappa d}\cosh(\lambda_{sl}d)\left(1+\frac{\kappa}{\lambda_{sl}}\tanh(\lambda_{sl}d)\right)\right\}+\left(\frac{\kappa}{\lambda_{sl}}\right)^2\left(1-\frac{1}{F_1}\right)+$$
$$\frac{\lambda_{sl}}{\lambda_c}\coth(\lambda_c L/2)\frac{1}{F_1}\left\{\left(\frac{\kappa^2}{\kappa^2-\lambda_{sl}^2}\right)\sinh(\lambda_{sl}d)-\frac{\kappa\lambda_{sl}}{\kappa^2-\lambda_{sl}^2}\sinh(\kappa d)+\right.$$
$$\left.\left.\frac{P\kappa\lambda_{sl}}{\kappa^2-\lambda_{sl}^2}\left(1-\mathrm{e}^{-\kappa d}\cosh(\lambda_{sl}d)\left(1+\frac{\lambda_{sl}}{\kappa}\tanh(\lambda_{sl}d)\right)\right)\right\}\right]+\frac{\rho_{core}}{\eta\kappa^2}Q\frac{F_2}{F_1}+ \tag{28}$$
$$\frac{\rho_{core}}{\eta\kappa^2}Q\frac{1}{F_1}\frac{\lambda_{sl}^2}{\kappa^2-\lambda_{sl}^2}\left[1-\mathrm{e}^{-\kappa d}\cosh(\lambda_{sl}d)\left(1+\frac{\kappa}{\lambda_{sl}}\tanh(\lambda_{sl}d)\right)\right]+$$
$$\frac{\rho_{core}}{\eta\kappa\lambda_c}Q\frac{1}{F_1}\frac{\lambda_{sl}^2}{\kappa^2-\lambda_{sl}^2}\left(1-\mathrm{e}^{-\kappa d}\cosh(\lambda_{sl}d)\left(1+\frac{\lambda_{sl}}{\kappa}\tanh(\lambda_{sl}d)\right)\right)+$$
$$\frac{\rho_{core}}{\eta\kappa^2}\frac{1}{F_1}(1-F_2)+\frac{\rho_{core}}{\eta\lambda_c^2}\frac{1}{F_1}$$

, where the scalars $F_{1,2}$ are defined by

$$\begin{cases} F_1 = \cosh(\lambda_{sl}d)+(\lambda_{sl}/\lambda_c)\coth(\lambda_c L/2)\sinh(\lambda_{sl}d) \\ F_2 = \dfrac{1-(\kappa/\lambda_c)\coth(\lambda_c L/2)\tanh(\kappa L/2)}{1-\kappa^2/\lambda_c^2} \end{cases} \tag{29}$$

Equation (28) is one of key results of this study. For $\kappa >> 1$ reached at sufficiently large electrolyte concentrations, the electrophoretic mobility expression (28) reduces to the non-zero mobility value, given by

$$\mu_E = \frac{\rho_{shell}}{\eta\lambda_{sl}^2}\left(1-\frac{1}{F_1}\right)+\frac{\rho_{core}}{\eta\lambda_c^2}\frac{1}{F_1} \tag{30}$$

The above expression is valid for any arbitrary choice of $\lambda_c L$ and $\lambda_{sl}d$. This non-zero mobility plateau value is the specific signature for the presence of flow-permeable shell and core particle components [1] and Eq. (30) makes explicit their respective contributions in defining the overall particle mobility under conditions where particle electrostatics is completely screened. It is recalled here that the mobility of hard particles at infinite ionic strength, unlike that of their soft counterparts, is necessarily zero due to electric double layer screening effect [2, 19, 20]. It is noted that the existence of a non-zero mobility for a soft core-shell particle at large electrolyte concentrations can be equally demonstrated from the balance between the frictional force $-\gamma_{c,sl}u(x)$ exerted by the particle shell on the flow and the driving electric force acting on the fixed charges supported by the polymer backbone constituting the inner core and the

outer PEL particle components [46]. If we further consider $\lambda_c^{-1} \to 0$ reflecting the absence of flow in the particle core region, the mobility expression (30) reduces to

$$\mu_E = \frac{\rho_{shell}}{\eta \lambda_{sl}^2}\left(1 - \frac{1}{\cosh(\lambda_{sl} d)}\right) \tag{31}$$

, which is identical to Eq. (11.6.4) given in [25] by Ohshima and to the result provided in [58] for the situation of a hard core-Ssl particle at sufficiently large electrolyte concentrations. On the other hand, in the limits where dimensions of core and shell largely exceed their defining Brinkman lengths, *i.e.* $\lambda_c L >> 1$ and $\lambda_{sl} d >> 1$, and further considering cases where Donnan potentials are reached in the core and shell regions, *i.e.* $\kappa L >> 1$ and $\kappa d >> 1$, Eq. (28) reduces to the simple form

$$\mu_E = \frac{\varepsilon_e}{\eta}\left[\frac{\psi(0)/\kappa + \psi_{DON}/\lambda_{sl}}{1/\kappa + 1/\lambda_{sl}}\right] + \frac{\rho_{shell}}{\eta \lambda_{sl}^2} \tag{32}$$

Under such conditions, the value of the interfacial potential $\psi(0)$ is given by $\psi(0) = \psi_{DON}/2$. In turn, the above expression (32) identifies with the pioneering result derived by Ohshima [25] (Eq. (11.4.18) therein, taken in the limit of low Donnan potentials). Interestingly, the above mobility expression does not involve any electrostatic nor hydrodynamic contributions stemming from the inner PEL core region. Indeed, under the conditions underlying applicability of Eq. (32), the outer PEL shell with thickness well above the Debye and Brinkman lengths fully screen both electrostatic and hydrodynamic contributions of the inner core particle component and thus solely determines the particle electrophoretic behavior. If we further take the limit of Eq. (32) at $\lambda_{sl} \to \infty$, which refers to a hydrodynamic friction by the PEL surface so large that the flow penetration inside it is insignificant, then Eq. (32) properly reduces to the well-known Smoluchowski equation [72] given by $\mu_E = \frac{\varepsilon_e}{\eta}\psi(0)$, where the potential $\psi(0) = \psi_{DON}/2$ then identifies with the particle zeta-potential [2,19].

For cases where Brinkman lengths defining core and shell permeabilities to flow are well above the Debye length (*i.e.* $\kappa >> \lambda_{sl}$ and $\kappa >> \lambda_c$), Eq. (28) yields

$$\mu_E = \frac{\rho_{shell}}{\eta \lambda_{sl}^2}\left[1 - \frac{1}{\cosh(\lambda_{sl} d)}\right] + \frac{\rho_{core}}{\eta \lambda_c^2}\frac{1}{\cosh(\lambda_{sl} d)} \tag{33}$$

, which correctly compares with the result given by Duval and Ohshima [58] in the specific limit where particle core is impermeable to flow (*i.e.* $\lambda_c \to \infty$). Eq. (33) further reduces to the following simplified expression valid for sufficiently large core and large shell sizes as compared to the core and shell Brinkman lengths (*i.e.* $\lambda_c L >> 1$ and $\lambda_{sl} d >> 1$, respectively)

$$\mu_E = \frac{\rho_{shell}}{\eta \lambda_{sl}^2} \tag{34}$$

, which is nothing else than the second term of Eq. (32) reached at sufficiently large electrolyte concentrations where $\psi_{DON} \to 0$.

The electrophoretic mobility expression for composite particles defined by a shell layer surrounding a core that is **not** permeable to fluid flow (this concerns all particles types given in **Table 1**, at the exception of the Sc-Ssl particles situation treated above, see Eq. (28)) is obtained from the mobility expression applicable to Sc-Ssl particles taken in the limit of infinite hydrodynamic softness within the particle core component (*i.e.* $\lambda_c^{-1} \to 0$, Eq. (S15) in **Supplementary Material**). In turn, we obtain

$$\mu_E = \frac{\varepsilon_e}{\eta} \frac{1}{\cosh(\lambda_{sl} d)} \left[\psi(-d) + \lambda_{sl} \int_{-d}^{0} \psi(x) \sinh\left[\lambda_{sl}(x+d)\right] \mathrm{d}x \right] + \frac{\varepsilon_e}{\eta} \left(\frac{\kappa}{\lambda_{sl}} \right)^2 \psi_{DON} \left[1 - \frac{1}{\cosh(\lambda_{sl} d)} \right] \tag{35}$$

, which is thus valid for **SSc-Ssl, hard core-Ssl, hard core-SSsl** and **SSc-SSsl** particle types (**Table 1**) pending replacement of the potential distribution $\psi(x)$ in Eq. (35) by its appropriate defining expression in line with the particle type considered (see §2.2.2 and §2.2.3). In particular, substitution of $\psi(x)$ given by Eq. (22) into Eq. (35) leads after calculation to the following expression for the electrophoretic mobility of **SSc-Ssl** particles

$$\begin{aligned} \mu_E = \frac{\varepsilon_e}{\eta} \psi_{DON} \Bigg[& \frac{\kappa^2}{\kappa^2 - \lambda_{sl}^2} \left(1 - \frac{\cosh(\kappa d)}{\cosh(\lambda_{sl} d)} \right) + P \left(\frac{\kappa^2}{\kappa^2 - \lambda_{sl}^2} \frac{1}{\cosh(\lambda_{sl} d)} - \frac{\lambda_{sl}^2}{\kappa^2 - \lambda_{sl}^2} \mathrm{e}^{-\kappa d} \left(1 + \frac{\kappa}{\lambda_{sl}} \tanh(\lambda_{sl} d) \right) \right) \\ & + \frac{\kappa^2}{\lambda_{sl}^2} \left\{ 1 - \frac{1}{\cosh(\lambda_{sl} d)} \right\} \Bigg] + \frac{\rho_{core}}{\eta \kappa^2} Q \left[\frac{\kappa^2}{\kappa^2 - \lambda_{sl}^2} \frac{1}{\cosh(\lambda_{sl} d)} - \frac{\lambda_{sl}^2}{\kappa^2 - \lambda_{sl}^2} \mathrm{e}^{-\kappa d} \left(1 + \frac{\kappa}{\lambda_{sl}} \tanh(\lambda_{sl} d) \right) \right] \end{aligned} \tag{36}$$

, where P and Q are defined by Eq. (23).

For the classical hard core-soft shell particle configuration (**hard core-Ssl** particle, **Table 1**) the inner core is impermeable to both ions and fluid flow. For such a particle type, the substitution of the potential distribution defined by Eq. (25) into Eq. (35) yields, after some rearrangements, to the following expression of the electrophoretic mobility μ_E

$$\begin{aligned} \mu_E = \frac{\varepsilon_e}{\eta} \psi_{DON} \Bigg[& 1 + \frac{\lambda_{sl}^2}{2(\kappa^2 - \lambda_{sl}^2)} \left(1 + \mathrm{e}^{-2\kappa d} - \frac{\kappa}{\lambda_{sl}} (1 - \mathrm{e}^{-2\kappa d}) \tanh(\lambda_{sl} d) \right) - \frac{\kappa^2}{\kappa^2 - \lambda_{sl}^2} \frac{\mathrm{e}^{-\kappa d}}{\cosh(\lambda_{sl} d)} \\ & + \frac{\kappa^2}{\lambda_{sl}^2} \left\{ 1 - \frac{1}{\cosh(\lambda_{sl} d)} \right\} \Bigg] + \frac{\rho_{core} L}{2 \eta \kappa} \left[\frac{\kappa^2}{\kappa^2 - \lambda_{sl}^2} \frac{1}{\cosh(\lambda_{sl} d)} - \frac{\lambda_{sl}^2}{\kappa^2 - \lambda_{sl}^2} \mathrm{e}^{-\kappa d} \left(1 + \frac{\kappa}{\lambda_{sl}} \tanh(\lambda_{sl} d) \right) \right] \end{aligned} \tag{37}$$

The first term in Eq. (37) involves the Donnan potential ψ_{DON} and corresponds to the contribution of the shell charge density to the particle electrophoretic mobility. The second term involving ρ_{core} stems from the contribution of the charges distributed in the particle core volume. For a **hard core-Ssl** particle with uncharged inner core ($\rho_{core} = 0$) supporting a charged soft layer, the mobility expression given in Eq. (37) becomes identical to Eq. (56) given in [54]. In the limit $L \to 0$ and $\rho_{core} \to \infty$ with the product $L\rho_{core}/2$ kept constant, $L\rho_{core}/2$ tends to the core surface charge density σ, and the second term on the right-hand side of Eq. (37) reduces to

$$\mu_E = \frac{\sigma}{\eta\kappa}\left[\frac{\kappa^2}{\kappa^2-\lambda_{sl}^2}\frac{1}{\cosh(\lambda_{sl}d)} - \frac{\lambda_{sl}^2}{\kappa^2-\lambda_{sl}^2}\mathrm{e}^{-\kappa d}\left(1+\frac{\kappa}{\lambda_{sl}}\tanh(\lambda_{sl}d)\right)\right] \tag{38}$$

, which agrees with the mobility expression derived in [53] (Eq. (30) therein) for a plate-like particle carrying a surface charge density σ coated by an uncharged polymer layer of thickness d . A simplified form of the electrophoretic mobility expression (37) in the limit $\kappa >> \lambda_{sl}$ is provided by Eq. (S18) in **Supplementary Material**, and it further reduces to Eq. (34) for $\lambda_{sl}d >> 1$. It may be noted that Eq. (32) first obtained by Ohshima [25] may be recovered from the limit of Eq. (37) at $\lambda_{sl}d >> 1$, $\kappa d >> 1$ and $\rho_{core} \to 0$. Analyzing Eq. (37) in the situation where there is no fluid flow in the peripheral particle shell layer (*i.e.* $1/\lambda_{sl} \to 0$), we obtain the mobility expression of **hard core-SSsl** particles (**Table 1**) that reads as

$$\mu_E = \frac{\varepsilon_e}{\eta}\frac{\psi_{DON}}{2}(1-\mathrm{e}^{-2\kappa d}) + \frac{\rho_{core}}{2\varepsilon_e\kappa}L\mathrm{e}^{-\kappa d} \tag{39}$$

For particles in line with Donnan distribution of the electrostatic potential, achieved for $\kappa d >> 1$, Eq. (39) further reduces to $\mu_E = \frac{\varepsilon_e}{\eta}\frac{\psi_{DON}}{2}$. This expression, once again, correctly identifies with the standard Smoluchowski equation [2, 19, 72] valid for flow/ions-impermeable particles with surface potential $\psi_{DON}/2$. This potential may be assimilated to a zeta-potential that is *a priori* introduced within hard surface electrokinetic theories without explicit connection to the bulk particle electrostatic features.

Finally, the mobility expression pertaining to **SSc-SSsl** particles (**Table 1**) is simply derived from that of **SSc-Ssl** particles (Eq. (36)) in the limit of infinite hydrodynamic softness within the particle shell component (*i.e.* $\lambda_{sl}^{-1} \to 0$), which in turn leads to

$$\mu_E = \frac{\varepsilon_e}{\eta}\left(\psi_{DON}P + Q\frac{\rho_{core}}{\varepsilon_e\kappa^2}\right)\mathrm{e}^{-\kappa d} \tag{40}$$

Similarly to the case of **hard core-SSsl** particles, expression (40) takes the form of the standard Smoluchowski equation [2, 19, 72] applied to flow-impermeable particles whose outer surface potential (or, equivalently, zeta potential) is defined by $\left(\psi_{DON}P + Q\frac{\rho_{core}}{\varepsilon_e\kappa^2}\right)\mathrm{e}^{-\kappa d}$. The latter expression illustrates the differentiated contributions of the charged inner core and of the outer shell region (both permeable to electrolyte ions in **SSc-SSsl** particle type) in defining the potential at the outer particle surface. These contributions depend here on the geometrical properties of the particle (L and d, both involved in the expressions of P and Q), on the electrolyte concentration and on the space charge densities operational in the core and shell domains. For cases where core and outer shell layer carry oppositely charged functional groups, the electrophoretic mobility of the particle then changes sign with varying the concentration of background electrolyte, and the underlying shift in point of zero mobility is generally also a function of the respective hydrodynamic softness of the core and of the shell particle components [6, 32, 39, 40].

As a summary of this section, the developed expressions for the electrophoretic mobility of **Sc-Ssl**, **SSc-Ssl**, **hard core-Ssl**, **hard core-SSsl** and **SSc-SSsl** composite particles are defined by Eqs. (28), (36), (37), (39) and (40), respectively. These expressions are the key results of this work.

2.4. Computational illustrations.

In this section, we discuss the dependence of the electrophoretic mobility of the composite core-shell particle types defined in **Table 1** on the respective magnitudes of the relevant electrostatic Debye layer thickness, hydrodynamic screening lengths, core diameter and shell thickness. Results are given in the dimensionless form μ_E / μ_0 with $\mu_0 = \varepsilon_e RT / (F\eta)$.

The scaled electrophoretic mobility of a **Sc-Ssl** particle (Eq. (28)) defined by core and shell regions that are both permeable to ions and fluid flow is shown in **Figure 2** as a function of the dimensionless product $\lambda_c L$, which reflects the ability of the core to host fluid flow, for various values of its equivalent for the shell layer, $\lambda_{sl} d$. The reader is referred to the caption of Figure 2 for details on selected model parameters. For the sake of comparison, the scaled electrophoretic mobility of **SSc-Ssl** particles derived from Eq. (36) is reported in **Figure 2**.

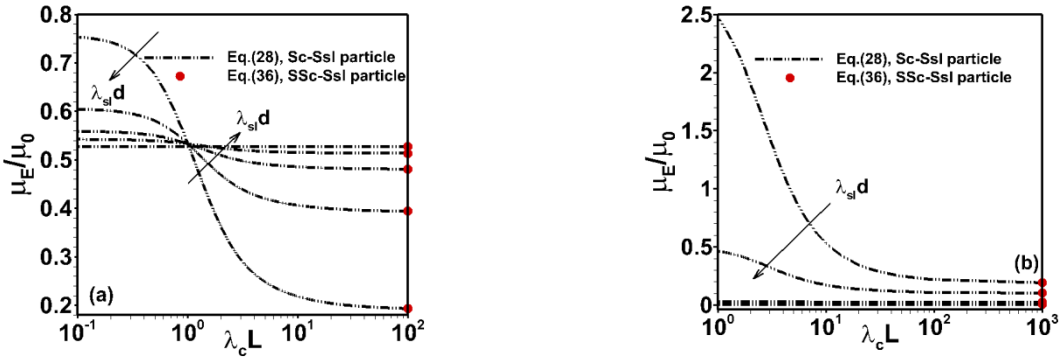

Fig. 2. Dependence of scaled electrophoretic mobility of **Sc-Ssl** particles (see **Table 1**, Eq. (28)) on dimensionless $\lambda_c L$ varied at fixed (a) $L = 10$ nm. Results are given for various values of $\lambda_{sl} d$ with λ_{sl}^{-1} =10 nm and d =10, 20, 30, 40, 200 nm (growing d values in the direction given by the arrows). (b) As in (a) with $L = 100$ nm, d =10 nm, and λ_{sl}^{-1} = 0.1, 1, 2, 5, 10 nm (growing $\lambda_{sl} d$ values in the direction given by the arrow). Other model parameters: $\rho_{shell} / z_{shell} F = \rho_{core} / z_c F = 1$ mM and $\kappa^{-1} = 1$ nm. For the sake of comparison, value of the electrophoretic mobility of **SSc-Ssl** particles obtained from Eq. (36) is further reported (red dots).

Figure 2 evidences a decrease of the **Sc-Ssl** particle electrophoretic mobility with increasing $\lambda_c L$, *i.e.* with decreasing the permeability of the particle core component to fluid flow at fixed inner core diameter (L=10 nm in **Figure 2a**). At sufficiently low $\lambda_c L$, the interaction between the applied electric field and the electric double layer developed within the charged core leads therein to a significant electroosmotic flow (EOF) of counterions. An increase of the dimensionless hydrodynamic softness $\lambda_c L$ of the core partly suppresses this EOF and thus results in an accumulation of counter-ions therein. In turn, upon increasing $\lambda_c L$ at fixed L, the net density of charges entrapped within the inner PEL core is reduced, which leads to decreasing electrophoretic mobility (in absolute value). At sufficiently large $\lambda_c L$ where core region becomes semi-soft (*i.e.* permeable to ions but impermeable to flow), μ_E / μ_0 approaches an asymptotic plateau value that correctly compares with prediction from Eq. (36) applicable to **SSc-Ssl** particle (**Figure 2a**). The dependence of that plateau value on $\lambda_{sl} d$ at fixed λ_{sl} is further consistent with evaluations from Eq. (36). Namely, increasing $\lambda_{sl} d$ at $\lambda_c L \to \infty$ and fixed λ_{sl} (*i.e.* d is increased) comes to add structural shell charges at the periphery of the particle core, which increases the potential locally in this particle region (as long as κd does not largely exceed unity), and this process gives rise to an increase in μ_E / μ_0. Conversely, at sufficiently low $\lambda_c L$ where core permeability to flow significantly contributes to μ_E / μ_0, any increase in d comes to significantly screen the dominant hydrodynamic contribution of the core, which reduces μ_E / μ_0. Altogether, the processes identified at low and large

$\lambda_c L$ lead to the remarkable dependence of μ_E / μ_0 on $\lambda_{sl} d$ and $\lambda_c L$ as pictured by **Figure 2a**. Similar trends are obtained with increasing L (all other parameters being similar to those in **Figure 2a**, results not shown), which mostly affects the mobility behavior at sufficiently low $\lambda_c L$ where flow in the particle core is more significant than that in **Figure 2a**. **Figure 2b** identifies conditions where the shell-mediated hydrodynamic screening of the core contribution to the overall particle mobility is operational over the whole range of $\lambda_c L$ tested.

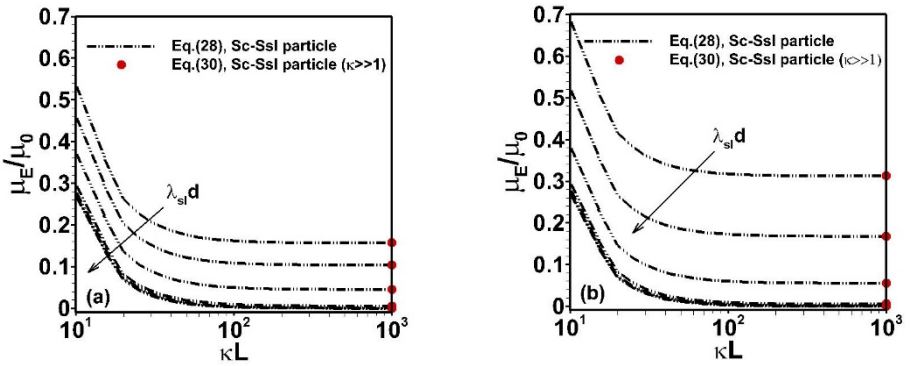

Fig. 3. Dependence of scaled electrophoretic mobility of **Sc-Ssl** particles obtained from Eq. (28) on dimensionless κL at fixed $L = 100$ nm, d = 10 nm with $\rho_{shell} / z_{shell} F = \rho_{core} / z_c F = 1$ mM, (a) λ_c^{-1} =1 nm, (b) λ_c^{-1} =10 nm and for various values of λ_{sl}^{-1} (= 0.1, 0.2, 0.5, 1, 2, 5, 10 nm) (growing $\lambda_{sl} d$ values in the direction given by the arrows). For the sake of comparison, value of the electrophoretic mobility of **Sc-Ssl** particles in the limit of infinite electrolyte concentrations (Eq. (30)) is further reported (red dots).

Figure 3 illustrates the impact of the electric double layer thickness, here expressed in terms of the dimensionless number κL, on the electrophoretic mobility of **Sc-Ssl** particles (Eq. (28). The limiting electrophoretic behavior of these particles at infinite ionic strengths ($\kappa \to \infty$), captured by Eq. (30), is further reported. In line with anticipation, results indicates that increasing the extent of screening of the overall particle charge (increasing κL) leads to a decrease in scaled mobility μ_E / μ_0 and a correct convergence of Eq. (28) to Eq. (30) at $\kappa L >> 1$. **Figure 3** further makes it clear that μ_E / μ_0 approaches a non-zero plateau value at $\kappa L >> 1$, a feature that is the characteristic signature of electroosmotic flow penetration in the charged particle body. At given κL, μ_E / μ_0 further decreases with increasing the scaled hydrodynamic softness parameters $\lambda_{sl} L$ and $\lambda_c L$ pertaining to the shell (**Figures 3a,b**) and to the core (**Figure 3b *vs.* 3a**), respectively, and the underlying reasons are similar to those already invoked for discussion of the results in **Figure 2**.

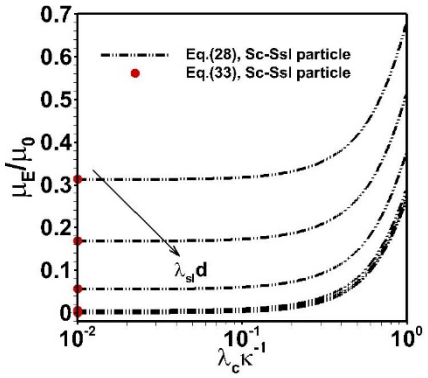

Fig. 4. Dependence of scaled electrophoretic mobility of **Sc-Ssl** particles obtained from Eq. (28) on dimensionless $\kappa^{-1}/\lambda_c^{-1}$ at fixed λ_c^{-1} = 10 nm with $\rho_{shell}/z_{shell}F = \rho_{core}/z_cF = 1$ mM, d = 10 nm, $L = 100$ nm and λ_{sl}^{-1} =0.1, 0.2, 0.5, 1, 2, 5, 10 nm (growing $\lambda_{sl}d$ values in the direction given by the arrow). For the sake of comparison, the value of the electrophoretic mobility of **Sc-Ssl** particles obtained from Eq. (33) is further reported (red dots).

Figure 4 shows how the scaled electrophoretic mobility of **Sc-Ssl** particles (Eq. (28)) is impacted by the extension of the electric double layer as compared to the inner PEL hydrodynamic screening length λ_c^{-1}. Like in **Figures 2-3**, results are given for various values of $\lambda_{sl}d$. At fixed $\lambda_{sl}d$, μ_E/μ_0 increases with increasing $\lambda_c\kappa^{-1}$ at fixed λ_c^{-1} due to reduction of the particle charge screening by ions from the background electrolyte. The non-zero plateau value reached by the electrophoretic mobility at infinite EDL screening ($\kappa >> \lambda_{sl}$ and $\kappa >> \lambda_c$), given by Eq. (33), is reached at sufficiently small $\lambda_c\kappa^{-1}$ for which the EDL thickness is far smaller than the hydrodynamic screening length of the inner PEL core. For increasing values of the hydrodynamic screening length of the inner PEL at fixed κ, the screening of the EOF in the core particle region is necessarily lesser pronounced and a similar feature occurs when increasing κ^{-1} at fixed λ_c, *i.e.* with increasing $\lambda_c\kappa^{-1}$. In turn, this leads to an increase in particle electrophoretic mobility. As expected from the results given in **Figure 2b**, increase of $\lambda_{sl}d$ at fixed d for particles with significant inner EOF leads to enhanced screening of the EOF developed within the outer PEL shell and therefore to a reduction in particle mobility.

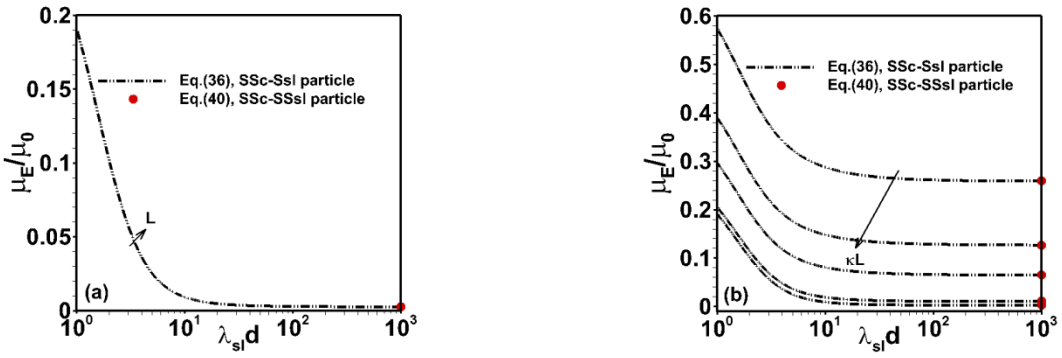

Fig. 5. Dependence of scaled electrophoretic mobility of **SSc-Ssl** particles obtained from Eq. (36) on dimensionless $\lambda_{sl}d$ for d =10 nm, with $\rho_{shell}/z_{shell}F = \rho_{core}/z_cF = 1$ mM. The results are shown for (a) κ^{-1} =1 nm at various values of L = 10, 50, 100, 200, 500 nm (growing L values in the direction given by the arrow). In panel (b), results are given for various values of κL at fixed L =100 nm. For the sake of comparison, the value of the electrophoretic mobility of **SSc-SSsl** particles obtained from Eq. (40) is further reported (red dots).

The dependence of the electrophoretic mobility of **SSc-Ssl** particles on $\lambda_{sl}d$ is provided in **Figure 5** at different electrolyte concentrations (or κ) and different choices of inner PEL core diameter L. At sufficiently large values of $\lambda_{sl}d$ where flow penetration into the particle shell region is insignificant, all results satisfactorily merge with predictions obtained for **SSc-SSsl** particles (Eq. (40)). While the effect of $\lambda_{sl}d$ on μ_E/μ_0 conforms to that discussed in previous figures (screening of the EOF in the shell layer), **Figure 5a** further illustrates that the electrophoretic mobility becomes independent of the size L of the inner particle core at sufficiently thin electric double layers as compared to L. This finding simply reflects that the potential distribution across the core/shell/solution interphase becomes unaffected by changes in L pending the condition for achievement of Donnan potential in the core region (the maximum value the potential can reach therein) is respected, *i.e.* the inequality $\kappa L >> 1$ is satisfied, which holds in **Figure 5a**. This feature, combined with the fact that there is no flow inside the core region (a defining property of SSc-Ssl particles) results in an electrophoretic mobility that is independent of L under conditions of **Figure 5a**. Obviously, decreasing the value of κL *via* increasing $1/\kappa$ leads to stronger variations of μ_E/μ_0 with L (not shown) as the potential distribution inside the core then deviates from that dictated by the limit pictured by the Donnan representation. Doing so, the mobility increases with L as the potential in the bulk core region locally increases to reach Donnan value, and it becomes again independent of L for $\kappa L >> 1$. Making the analogy with Eq. (21), value of that Donnan potential in the particle core domain is given by $\rho_{core}/\varepsilon_e\kappa^2$. Finally, **Figure 5b** confirms the decrease in particle mobility when increasing particle charge screening through increasing κ at fixed L. Remarkably, at sufficiently large $\lambda_{sl}d$ and $\kappa L >> 1$, particle mobility tends to zero because of complete screening of the EDL and of absence of significant EOF in the shell layer. In this regime, the particle effectively behaves

as a hard particle with an outer surface potential that is determined by the electrolyte concentration and by the respective geometrical and electrostatic properties of the core and of the shell particle components according to $\left(\psi_{DON}P + Q\frac{\rho_{core}}{\varepsilon_e\kappa^2}\right)\mathrm{e}^{-\kappa d}$ (see Eq. (40)).

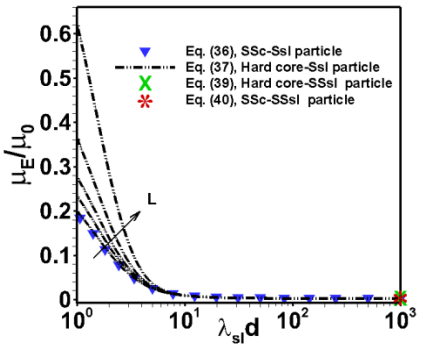

Fig. 6. Dependence of scaled electrophoretic mobility of **SSc-Ssl** and **hard core-Ssl** particles obtained from Eq. (36) and (37), respectively, on $\lambda_{sl}d$ for fixed d = 10 nm, κ^{-1} =1 nm with $\rho_{shell}/z_{shell}F = \rho_{core}/z_cF = 1$ mM and different L = 10, 50, 100, 200, 500 nm. For the sake of comparison, the value of the electrophoretic mobility of **hard core-SSsl** and **SSc-SSsl** particles obtained from Eq. (39) and Eq. (40), respectively, are reported.

Differences in the electrophoretic behavior of **SSc-Ssl** and **hard core-Ssl** particles are reported in **Figure 6**. Following their definition (**Table 1**), the former allows penetration of ions but not flow in the inner particle core, whereas the latter is impermeable to both ions and flow. It is found that the electrophoretic mobility of **hard core-Ssl** particles depends on the particle inner core size at sufficiently low values of $\lambda_{sl}d$ where the hydrodynamic Brinkman length of the outer shell layer is significantly large compared to d. On the opposite, the inner core size has basically no impact on μ_E/μ_0 of **SSc-Ssl** particles as Donnan potential conditions in the core region are met in **Figure 6** (see discussion of **Figure 5**). For **hardcore-Ssl** particles, the electrostatic potentials increase significantly at the core/shell interface with increasing L, which leads to a significant increment in particle mobility. For both types of particles, increasing $\lambda_{sl}d$ comes to an efficient screening of the EOF through the outer PEL and this leads to a reduction in electrophoretic mobility, as discussed previously. We also find that for sufficiently large values of $\lambda_{sl}d$, the mobility of **SSc-Ssl** particles identifies with that of **hard core-Ssl** particles, regardless of L. This is so because for such magnitude of $\lambda_{sl}d$, the electro-hydrodynamic contribution of the core to the overall particle mobility is completely screened by the flow-impermeable shell layer, whether the core is semi-soft or hard in nature. In line with expectation, the value of the mobility reached by **SSc-Ssl** and **hard core-Ssl** particle types at $\lambda_{sl}d \to \infty$ equates that of **SSc-SSsl** and **hardcore-SSsl** particles (Eqs. (40) and

(39), respectively) as the outer particle shell layer then transitions from soft to semi-soft layer type. For the sake of completeness, **Figure S1** in **Supplementary Material** further illustrates the expected limitations of Eq. (32), first derived by Ohshima [25], in capturing the electrophoretic behavior of various composite soft/semi-soft core-shell particle types at low values of $\lambda_{sl}d$.

3. Conclusions

In this study, we report an original analytical expression (Eq. (28)) for the electrophoretic mobility of a generic type of core-shell particles where core and shell components are defined by differentiated permeabilities to ions and fluid flow. Limits of this expression further lead to the elaboration of expressions, so-far missing from literature, applicable to soft core-soft shell, semi-soft core-soft shell, semi-soft core-semi-soft shell particles where the terminology 'semi-soft' refers to particle regions permeable to ions **but not** to fluid flow, and the qualification 'soft' applies to particle domains permeable to both ions and fluid flow. The theory is developed for particulate systems in line with the applicability of the thin double layer approximation within the framework of the linearized Poisson-Boltzmann formalism, valid at sufficiently large electrolyte concentrations and poorly to modestly particle core and shell components. Additional limits of our generic electrophoretic mobility expression considered for specific ranges of particle core diameter, shell dimension, electrolyte concentration and magnitude of flow permeabilities are shown to recover analytical results from literature, most of them derived by Ohshima [25, 51-54]. These limits include the historical case of hard particles with clearly established zeta potential concept [2, 19, 72], and that of hard core-soft shell particle [54]. Computational examples further illustrate that our expression is valid over a wider range of electrolyte concentrations, particle sizes and Brinkman length scales as compared to the analytical results given in [25, 51-54]. Altogether, this work provides a rather complete taxonomic survey of particle structure-electrophoresis relationships *via* in-depth analysis of the mobility expression developed here for the most generic and complex situation of soft core-soft shell particles. In particular, the results favor the quantitative identification of the respective electro-hydrodynamic contributions of the core and shell compartments to overall particle electrophoretic mobility, depending on core and shell sizes, on electrolyte concentration in solution, on the space charge densities operational in the core and shell volume and on their respective Brinkman hydrodynamic screening length scales.

There is now a large body of work [29, 30, 60-65, 73] where experimental electrophoretic mobility data, measured *e.g.* on microorganisms, nanoparticles or colloids, are interpreted on the basis of analytical equations derived by Ohshima valid for specific ranges of particle size, Debye layer thickness and shell Brinkman length. It is believed that the analytical mobility expressions developed here, valid over a larger range of conditions and applicable to a wider spectrum of core-shell particle types, will pave the way for a

refined evaluation of the electro-hydrodynamic properties of colloids whose composition often involves complex mixtures of biotic and abiotic materials with diversified (bio)polymers-based surface functionalization, as required in drug delivery [74], environmental [75] and other biomedical applications [76-77]. Future developments of this work involve the derivation of electrophoretic mobility of the composite core-shell particles examined here *albeit* with full account of electric double layer relaxation and polarization at the Poisson-Nernst-Planck level, which requires numerical analysis of the relevant governing electro-hydrodynamic equations. Comparison of such results with existing numerical theories [39, 48-50, 58] and predictions derived from the here-established analytical expressions will be useful to appreciate the extent by which these phenomena impact particle electrophoretic mobility depending on electrolyte concentration, particle core size, shell layer thickness, ions- and flow-permeabilities of the respective core and shell particle compartments. Relevant experimental data analysis by means of our generalized mobility expression (Eq. (28)) requires (i) particle mobility measurements performed over a broad range of pH and/or salt concentration conditions in order to constrain the confrontation between experiments and theory and, as mentioned above, (ii) a comparison with the outcome from exact numerical theory, the conditions (i) and (ii) being necessary to properly determine either the magnitude of the various electrohydrodynamic parameters involved in the problem (especially the charges and flow permeabilities of the particle core and shell compartments) or any relevant combinations thereof.

Funding P.P. Gopmandal kindly acknowledges the financial support by the Science and Engineering Research Board, Department of Science & Technology, Government of India, through the project grant File no. MTR/2018/001021.

Supplementary Material. 1. Details on the derivation of the potential distribution relevant for a core-shell particle with ion-penetrable (1.1) and ion-impenetrable core (1.2) component (Eqs. (S1)-(S10)). **2.** Details on the derivation of electroosmotic flow field and electrophoretic mobility expressions for Sc-Ssl particles type, and limits thereof (Eqs. (S11)-(S19)). **3.** Further illustration of the limits of Eq. (32) at low values of $\lambda_{sl}d$ and comparison to Eq. (28). The code for performing computations is available on request.

References

1. J.F.L. Duval, F. Gaboriaud, Progress in electrohydrodynamics of soft microbial particle interphases, Curr. Opin. Colloid Interface Sci. 15 (2010) 184-195.

2. A.V. Delgado, F. González-Caballero, R.J. Hunter, L.K. Koopal, J. Lyklema, Measurement and interpretation of electrokinetic phenomena, J. Colloid Interface Sci. 309 (2007) 194-224.

3. S.C. Nichols, M. Loewenberg, R.H. Davis, Electrophoretic particle aggregation, J. Colloid Interface Sci.. 176 (1995) 342-351.

4. A. Beaussart, C. Beloin, J.-M. Ghigo, M.-P. Chapot-Chartier, S. Kulakauskas, J.F.L. Duval, Probing the influence of cell surface polysaccharides on nanodendrimer binding to Gram-negative and Gram-positive bacteria using single-nanoparticle force spectroscopy, Nanoscale 10 (2018) 12743-12753.
5. A. Jacquot, C. Sakamoto, A. Razafitianamaharavo, C. Caillet, J. Merlin, A. Fahs, J.M. Ghigo, J.F.L. Duval, C. Beloin, G. Francius, The dynamics and pH-dependence of Ag43 adhesins' self-association probed by atomic force spectroscopy, Nanoscale 6 (2014) 12665-12681.
6. A. Beaussart, C. Caillet, I. Bihannic, R. Zimmermann, J.F.L. Duval, Remarkable reversal of electrostatic interaction forces on zwitterionic soft nanointerfaces in a monovalent aqueous electrolyte: an AFM study at the single nanoparticle level, Nanoscale 10 (2018) 3181-3190.
7. E. Kłodzińska, M. Szumski, E. Dziubakiewicz, K. Hrynkiewicz, E. Skwarek, W. Janusz, B. Buszewski, Effect of zeta potential value on bacterial behavior during electrophoretic separation, Electrophoresis 31 (2010) 1590-1596.
8. A. Kishida, H. Iwata, Y. Tamada, Y. Ikada, Cell behavior on polymer surfaces grafted with non-ionic and ionic monomers, Biomaterials 12 (1991) 786-792.
9. M.C. van Loosdrecht, J. Lyklema, W. Norde, G. Schraa, A.J. Zehnder, Electrophoretic mobility and hydrophobicity as a measured to predict the initial steps of bacterial adhesion, Appl. Environ. Microbiol. 53 (1987) 1898-1901.
10. R.M. Town, van H.P. Leeuwen, J.F.L. Duval, Rigorous physicochemical framework for metal ion binding by aqueous nanoparticulate humic substances: implications for speciation modelling by the NICA-Donnan and WHAM codes, Environ. Sci. Technol. 53 (2019) 8516-8532.
11. J.P.S. Sagou, E. Rotureau, F. Thomas, J.F.L. Duval, Impact of metallic ions on electrohydrodynamics of soft colloidal polysaccharides, Colloids Surf. A Physicochem. Eng. Asp. 435 (2013) 16-21.
12. J.F.L. Duval, J.P.S. Farinha, J.P. Pinheiro, Impact of electrostatics on the chemodynamics of highly charged metal-polymer nanoparticle complexes, Langmuir 29 (2013) 13821-13835.
13. R.J. Hill, Electrokinetics of nanoparticle gel-electrophoresis, Soft Matter 12 (2016) 8030-8048.
14. M. Elimelech, M. Nagai, C.-H. Ko, J.N. Ryan, Relative insignificance of mineral grain zeta potential to colloid transport in geochemically heterogeneous porous media, Environ. Sci. Technol. 34 (2000) 2143-2148.
15. M. Elimelech, C.R. O'Melia, Kinetics of deposition of colloidal particles in porous media, Environ. Sci. Technol. 24 (1990) 1528-1536.
16. J.F.L. Duval, Dynamics of metal uptake by charged biointerphases: bioavailability and bulk depletion, Phys. Chem. Chem. Phys. 15 (2013) 7873-7888.

17. C. Pagnout, R.M. Présent, P. Billard, E. Rotureau, J.F.L. Duval, What do luminescent bacterial metal-sensors probe? Insights from confrontation between experiments and flux-based theory, Sensors and Actuators B: Chemical 270 (2018) 482-491.

18. J.F.L. Duval, C. Pagnout, Decoding the time-dependent response of bioluminescent metal-detecting whole-cell bacterial sensors, ACS Sens. 4 (2019) 1373-1383.

19. J. Lyklema, Fundamentals of Interfaces and Colloid Science, vol. II, Academic Press, New York, 1995.

20. R.J. Hunter, Zeta Potential in Colloid Science, Academic Press, New York, 1981.

21. R.W. O'Brien, L.R. White, Electrophoretic mobility of a spherical colloidal particle, J. Chem. Soc. Faraday Trans. 2 74 (1978) 1607-1626.

22. J. Lyklema, Surface conduction, J. Phys. Condens. Matter 13 (2001) 5027-5034.

23. S. Bhattacharyya, P. P. Gopmandal, Migration of a charged sphere at an arbitrary velocity in an axial electric field, Colloids Surf. A Physicochem. Eng. Asp. 390 (2011) 86-94.

24. J.-P. Hsu, Z.-S. Chen, Electrophoresis of a sphere along the axis of a cylindrical pore: effects of double-layer polarization and electroosmotic flow, Langmuir 23 (2007) 6198-6204.

25. H. Ohshima, Electrophoresis of soft particles, Adv. Colloid Interface Sci. 62 (1995) 189-235.

26. Y. Maki, K. Sugawara, D. Nagai, Temperature dependence of electrophoretic mobility and hydrodynamic radius of microgels of poly(N-isopropylacrylamide), Gels 4 (2018) 37.

27. A. Fernandez-Nieves, M Márquez, Electrophoresis of ionic microgel particles: from charged hard spheres to polyelectrolyte-like behavior, J. Chem. Phys. 122 (2005) 84702.

28. S.M. Louie, T. Phenrat, M.J. Small, R.D. Tilton, G.V. Lowry, Parameter identifiability in application of soft particle electrokinetic theory to determine polymer and polyelectrolyte coating thicknesses on colloids, Langmuir 28 (2012) 10334-10347.

29. R. Sonohara, N. Muramatsu, H. Ohshima, and T. Kondo, Difference in surface properties between Escherichia coli and Staphylococcus aureus as revealed by electrophoretic mobility measurements, Biophys. Chem. 5 (1995) 273-277.

30. R. Bos, H.C. van der Mei, H.J. Busscher, 'Soft-particle' analysis of the electrophoretic mobility of a fibrillated and non-fibrillated oral streptococcal strain: Streptococcus salivarius, Biophys. Chem. 74 (1998) 251-255.

31. J.F.L. Duval, H.J. Busscher, B. van de Belt-Gritter, H.C. van der Mei, W. Norde, Analysis of the interfacial properties of fibrillated and non-fibrillated oral streptococcal strain from electrophoretic mobility and titration measurements: evidence for the shortcomings of the 'classical soft particle approach', Langmuir 21 (2005) 11268-11282.

32. J. Langlet, F. Gaboriaud, C. Gantzer, J.F.L. Duval, Impact of chemical and structural anisotropy on the electrophoretic mobility of spherical soft multilayer particles: the case of bacteriophage MS2, Biophys. J. 94 (2008) 3293-3312.

33. C. Dika, J.F.L. Duval, H.M. Ly, C. Merlin, C. Gantzer, Impact of internal RNA on aggregation and electrokinetics of viruses: comparison between MS2 phage and corresponding virus-like particles, Applied Environ. Microbiol. 77 (2011) 4939-4948.

34. J.R.S. Martin, I. Bihannic, C. Santos, J.P.S. Farinha, B. Demé, F.A.M. Leermakers, J.P. Pinheiro, E. Rotureau, J.F.L. Duval, Structure of multiresponsive brush-decorated nanoparticles: a combined electrokinetic, DLS, and SANS study, Langmuir 31 (2015) 4779-4790.

35. J. Lopez-Viota, S. Mandal, A.V. Delgado, J. L. Toca-Herrera, Moller Marco, F. Zanuttin, M. Balestrino, S. Krol, Electrophoretic characterization of gold nanoparticles functionalized with human serum albumin (HSA) and creatine, J. Colloid Interface Sci. 332 (2009) 215-223.

36. T.L. Doane, Y. Cheng, A. Babar, R.J. Hill, C. Burda, Electrophoretic mobilities of PEGylated gold NPs, J. Am. Chem. Soc. 132 (2010) 15624-15631.

37. N. Helfricht, E. Doblhofer, J. F. L. Duval, T. Scheibel, G. Papastavrou, Colloidal properties of recombinant spider silk protein particles, J. Phys. Chem. C. 120 (2016) 18015-18027.

38. J.F.L. Duval, K.J. Wilkinson, H.P. van Leeuwen, J. Buffle, Humic substances are soft and permeable: evidence from their electrophoretic mobilities, Environ. Sci. Technol. 39 (2005) 6435-6445.

39. M. Moussa, C. Caillet, R.M. Town, J.F.L. Duval, Remarkable electrokinetic features of charge-stratified soft nanoparticles: mobility reversal in monovalent aqueous electrolyte, Langmuir 31 (2015) 5656-5666.

40. J.F.L. Duval, C. Werner, R. Zimmermann, Electrokinetics of soft polymeric interphases with layered distribution of anionic and cationic charges, Curr. Opin. Colloid Interface Sci. 24 (2016) 1-12.

41. J.F.L. Duval, Electrophoresis of soft colloids: basic principles and applications. In Environmental Colloids and Particles: Behaviour, Separation and Characterization, Chapter 7. Eds. K.J. Wilkinson, J. Lead., Vol. 10 IUPAC series on Analytical and Physical Chemistry of Environmental Systems, Senior Editors J. Buffle and H.P. van Leeuwen, 2007.

42. H. Ohshima, Theory of Colloid and Interfacial Electric Phenomena, Volume 12, 1st Edition, Academic Press, 2006.

43. H. Ohshima, T. Kondo, Electrophoresis of large colloidal particles with surface charge layers. Position of the slipping plane and surface layer thickness, Colloid Polym. Sci. 264 (1986) 1080-1084.

44. H. Ohshima, T. Kondo, Electrophoretic mobility and Donnan potential of a large colloidal particle with a surface charge layer, J. Colloid Interface Sci. 116 (1987) 305-311.

45. H. Ohshima, T. Kondo, Approximate analytic expression for the electrophoretic mobility of colloidal particles with surface-charge layers, J. Colloid Interface Sci. 130 (1989) 281-282.
46. H. Ohshima, T. Kondo, On the electrophoretic mobility of biological cells, Biophys. Chem. 39 (1991) 191-198.
47. H. Ohshima, Theory of electrostatics and electrokinetics of soft particles, Sci. Technol. Adv. Mater. 10 (2009) 063001.
48. R.J. Hill, D.A. Saville, 'Exact' solutions of the full electrokinetic model for soft spherical colloids: electrophoretic mobility, Colloids Surf. A Physicochem. Eng. Asp. 267 (2005) 31-49.
49. J.J. Lopez-Garcia, C. Grosse, J. Horno, Numerical study of colloidal suspensions of soft spherical particles using the network method: 1. DC electrophoretic mobility, J. Colloid Interface Sci., 265 (2003) 327-340.
50. R.J. Hill, Hydrodynamics and electrokinetics of spherical liposomes with coatings of terminally anchored poly(ethylene glycol): numerically exact electrokinetics with self-consistent mean-field polymer, Phys. Rev. E 70 (2004) 051046.
51. H. Ohshima, Electrophoretic mobility of soft particle, J. Colloid Interface Sci. 163 (1994) 474-483.
52. H. Ohshima, On the general expression for the electrophoretic mobility of a soft Particle, J. Colloid Interface Sci. 228 (2000) 190-193.
53. H. Ohshima, Modified Henry function for the electrophoretic mobility of a charged spherical colloidal particle covered with an ion-penetrable uncharged polymer layer, J. Colloid Interface Sci. 252 (2002) 119-125.
54. H. Ohshima, Electrophoresis of soft particles: Analytic approximations, Electrophoresis 27 (2006) 526-533.
55. H. Ohshima, Electrophoretic mobility of a highly charged soft particle: Relaxation effect, Colloids Surf. A Physicochem. Eng. Asp. 376 (2011) 72-75.
56. U.K. Ghoshal, S. Bhattacharyya, P.P. Gopmandal, S. De, Nonlinear effects on electrophoresis of a soft particle and sustained solute release, Transport in Porous Med. 121 (2018) 121-133.
57. C. Cametti, Dielectric properties of soft particle in aqueous solutions, Soft Matter 7 (2011) 5494-5506.
58. J.F.L. Duval, H. Ohshima, Electrophoresis of diffuse soft particles, Langmuir 22 (2006) 3533-3546.
59. S.S. Dukhin, R. Zimmermann, J.F.L. Duval, C. Werner, On the applicability of the Brinkman equation in soft surface electrokinetics, J. Colloid Interface Sci. 350 (2010) 1-4.
60. S. Tsuneda, J. Jung, H. Hayashi, H. Aikawa, A. Hirata and H. Sasaki, Influence of extracellular polymers on electrokinetic properties of heterotrophic bacterial cells examined by soft particle electrophoresis theory, Colloids Surf. B: Biointerfaces 29 (2003) 181-188.

61. H. Hayashi, S. Tsuneda, A. Hirata, H. Sasaki, Soft particle analysis of bacterial cells and its interpretation of cell adhesion behaviors in terms of DLVO theory, Colloids Surf. B: Biointerfaces 22 (2001) 149-157.

62. H. Hayashi, H. Seiki, S. Tsuneda, A. Hirata and H. Sasaki, Influence of growth phase on bacterial cell electrokinetic characteristics examined by soft particle electrophoresis theory, J. Colloid Interface Sci. 264 (2003) 565-568.

63. K. Makino, H. Ohshima, Electrophoretic Mobility of a colloidal particle with constant surface charge density, Langmuir 26 (2010) 18016-18019.

64. J. Škvarla, D. Kupka, Y. Návesñáková, A. Škvarlová, An evaluation of the outer membrane charge and softness of Thiobacillusferrooxidans by the Ohshima's electrophoretic model of a "soft" particle, Folia Microbiologica 47 (2002) 218-224.

65. C. Pagnout, B. Sohm, A. Razafitianamaharavo, C. Caillet, M. Offroy, M. Leduc, H. Gendre, S. Jomini, A. Beaussart, P. Bauda, J.F.L. Duval, Pleiotropic effects of rfa-gene mutations on Escherichia coli envelope properties, Sci. Rep. (2019) 9:9696.

66. J. Lyklema, S. Rovillard, J. De Coninck, Electrokinetics: the properties of the stagnant layer unraveled, Langmuir 14 (1998) 5659-5663.

67. J. Lyklema, On the slip process in electrokinetics, Colloids Surf. A Physicochem. Eng. Asp. 92 (1994) 41-49.

68. L. Yezek, J.F.L. Duval, H.P. van Leeuwen, Electrokinetics of diffuse soft interfaces. III. Interpretation of data on the polyacrylamide/water interface, Langmuir 21 (2005) 6220-6227.

69. J.F.L. Duval, H.P. van Leeuwen, Electrokinetics of diffuse soft interfaces. I. Limit of low Donnan potentials, Langmuir 20 (2004) 10324-10336.

70. J.F.L. Duval, Electrokinetics of diffuse soft interfaces. II. Analysis based on the nonlinear Poisson-Boltzmann equation. Langmuir 21 (2005) 3247-3258.

71. S.K. Maurya, P.P. Gopmandal, S. Bhattacharyya, H. Ohshima, Ion partitioning effect on the electrophoresis of a soft particle with hydrophobic core, Phys. Rev. E. 98 (2018) 023103.

72. M. von Smoluchowski, Versucheiner Mathematischen Theorie der Koagulation Kinetic Kolloide Lousungen, J. Phys. Chem. C 92 (1917) 129-168.

73. A. Hyono, F. Gaboriaud, T. Mazda, Y. Takata, H. Ohshima, J.F.L. Duval, Impacts of papain and neuraminidase enzyme treatment on electrohydrodynamics and IgG-mediated agglutination of type A red blood cells, Langmuir 25 (2009) 10873-10885.

74. B. Fortuni, T. Inose, M. Ricci, Y. Fujita, I. Van Zundert, A. Masuhara, E. Fron, H. Mizuno, L. Latterini, S. Rocha, H. Uji-i, Polymeric engineering of nanoparticles for highly efficient multifunctional drug delivery systems, Sci. Rep. (2019) 9:2666.

75. F.D. Guerra, M.F. Attia, D.C. Whitehead, F. Alexis, Nanotechnology for environmental remediation: materials and applications, Molecules 23 (2018) 1760.
76. P.N. Navya, H.K. Daima, Rational engineering of physicochemical properties of nanomaterials for biomedical applications with nanotoxicological perspectives, Nano Converg. 3 (2016) 1.
77. J. Bacharouche, O. Erdemli, R. Rivet, B. Doucouré, C. Caillet, A. Mutschler, P. Lavalle, J.F.L. Duval, C. Gantzer, G. Francius, On the infectivity of bacteriophages in polyelectrolyte multilayer films: inhibition or preservation of their bacteriolytic activity? ACS Appl. Mater. Interfaces 10 (2018) 33545-33555.